PrePARED Report No. 14

Diel patterns in fish abundance and responses to bait within a commercial wind farm

PrePARED

Predators + Prey Around Renewable Energy Developments

University of Exeter

Funded by:

Offshore Wind Evidence + Change Programme

The Crown Estate

Crown Estate Scotland

Oighreachd a' Chrùin Alba

PrePARED Report

Diel patterns in fish abundance and responses to bait within a commercial wind farm

Samuel Gierhart, Mario Lambrette, Anthony W. Bicknell, Matthew J. Witt

University of Exeter, Hatherly Laboratories, Prince of Wales Road, Exeter, EX4 4PS, UK

Summary

- Unbaited stereo-camera seabed landers ("Cuttlefish") were deployed at the Beatrice Offshore Wind Farm in the Moray Firth, Scotland (19-26 July 2024), recording continuously at 30 m and 500 m from six turbine foundations. Haddock (*Melanogrammus aeglefinus*) and flatfish (common dab, *Limanda limanda* and European flounder, *Platichthys flesus*), the two most abundant taxa, were counted using machine-learning validated against a human annotator.

- Both taxa were approximately twice as abundant close to the foundations as 500 m away (haddock 2.3 times, flatfish 2.4 times), confirming a reef effect.

- Abundance varied through the day–night (diel) cycle, with lowest numbers in daylight and pronounced peaks at night and around dawn and dusk. The reef effect was consistent across all diel periods, applying both by day and by night.

- Comparison with concurrent Baited Remote Underwater Video (BRUV) deployments at 30 m revealed baited cameras recorded more fish than the unbaited landers (approximately 4 times more haddock and 2.6 times more flatfish), quantifying the influence of bait.

- Because abundance peaked at night, short daytime surveys may underestimate demersal fish use at turbine foundations. Covering six turbines over a single week, the patterns require confirmation through larger and repeated deployments but demonstrate that continuous monitoring reveals behaviour that conventional surveys cannot.

Recommended Citation

Gierhart, S., Lambrette, M., Bicknell, A. W. J., & Witt, M. J. (2026). Task 3.2. Work Package B – Diel patterns in fish abundance and responses to bait within a commercial wind farm. PrePARED Report, No. 014. July 2026.

Recommended Funding Acknowledgement

This work was funded by The Crown Estate Offshore Wind Evidence and Change (OWEC) Programme and Crown Estate Scotland. It is a component of the Predators and Prey Around Renewable Energy Developments (PrePARED) project.

This project forms part of the Offshore Wind Evidence and Change programme, led by The Crown Estate in partnership with the Department for Energy Security and Net Zero and Department for Environment, Food & Rural Affairs. The Offshore Wind Evidence and Change programme is an ambitious strategic research and data-led programme. Its aim is to facilitate the sustainable and coordinated expansion of offshore wind to help meet the UK's commitments to low carbon energy transition whilst supporting clean, healthy, productive and biologically diverse seas.

1. Introduction

The expansion of offshore wind energy has introduced artificial structures to the marine environment at an unprecedented scale, with thousands of turbines now operational or under construction in the North Sea alone (Reubens, Vandendriessche, et al., 2013). Turbine foundations provide hard substrate that can be colonised by marine communities and can alter the local abundance and behaviour of seabed-dwelling fish (demersal), which is broadly termed as the reef effect (Bergström et al., 2013; Degraer et al., 2020; ter Hofstede et al., 2022; Wilhelmsson et al., 2006). For demersal fish, higher abundance and biomass of both codfish (Gadidae) and flatfish (Pleuronectiformes) species have been recorded near foundations at North Sea wind farms (Bicknell et al., 2025; Buyse et al., 2022).

The evidence for the reef effect is frequently drawn from methods with short sampling durations, typically two hours or less. Assessments typically also rely on techniques conducted during daylight hours (Bicknell et al., 2019; Wilhelmsson et al., 2006). This is a potential limitation because activity and distribution are known to vary between day and night for demersal fish (Engås & Soldal, 1992; Løkkeborg et al., 1989; Petrakis et al., 2001), and acoustic telemetry has revealed dawn and dusk (i.e. crepuscular) movement patterns in Atlantic cod *Gadus morhua* at Belgian wind farm foundations linked to feeding activity (Reubens, Pasotti, et al., 2013). Whether the reef effect varies across the diel cycle has not been assessed, and daytime surveys, such as the concurrent BRUV survey at this site (Bicknell et al., 2026), may therefore capture only a partial picture of how fish use turbine structures.

Camera systems capable of recording for extended periods (e.g. many hours to days) offer an opportunity to address these temporal limitations, enabling characterisation of diel patterns in fish abundance that short-duration surveys cannot capture. Such deployments preclude the use of bait, which has a limited effective duration and cannot be replenished (Martinez et al., 2011), but in doing so also provide a means of comparing abundance counts between baited and unbaited approaches at the same site.

This study deployed custom-built unbaited camera systems at two distances from turbine jacket foundations at the Beatrice Offshore Wind Farm in the Moray Firth, Scotland, to investigate the effects of proximity to offshore wind turbines on fish abundance through day–night comparisons. Paired deployments of landers, at 30 m and 500 m from six turbine foundations, provided continuous recordings spanning daytime, crepuscular and nocturnal periods, enabling characterisation of diel patterns in fish abundance in the absence of bait, which is often considered a bias in baited camera surveys (Bicknell et al., 2019; Harvey et al., 2007).

The large volume of video data generated by these extended deployments was processed using a custom machine learning model trained for the automated detection of Gadidae and Pleuronectiformes species, providing a continuous, 1 second frequency, measure of abundance across the full recordings. While the model does not discriminate to species, concurrent baited remote underwater video (BRUV) surveys at this site recorded haddock (*Melanogrammus aeglefinus*) and dab and flounder as the dominant gadoid and flatfish taxa respectively (Bicknell et al., 2026), such that family-level detections can be reasonably interpreted as these species. The performance of this model was evaluated against manual annotation by a human observer.

Finally, a comparison of abundance, evaluated using MaxN, the maximum number of individuals of a species visible in a single frame and a widely used conservative estimate of abundance (Cappo et al., 2003; Willis & Babcock, 2000), was made between the unbaited landers and near-concurrent BRUV deployments. These were undertaken to evaluate the effect of bait on abundance estimates (Bicknell et al., 2026).

2. Methods

2.1 Study area

The study was performed at the Beatrice Offshore Wind Farm in the Moray Firth, Scotland, North Sea ([Fig. 1]), between 19–26 July 2024. The wind farm is located 7.5–12 nautical miles offshore (depth 35–60 m). Beatrice operates 84 (7 MW each) turbines with four-legged jacket foundations installed between August 2017 and July 2018; no scour protection on the seabed is present (Bicknell et al., 2025). The adjacent Moray East and Moray West wind farms are located to the south-east and south of Beatrice, respectively. Commercial fishing, including scallop dredging, trawling and creel potting, occurs within the wind farm boundaries (Dunkley & Solandt, 2022).

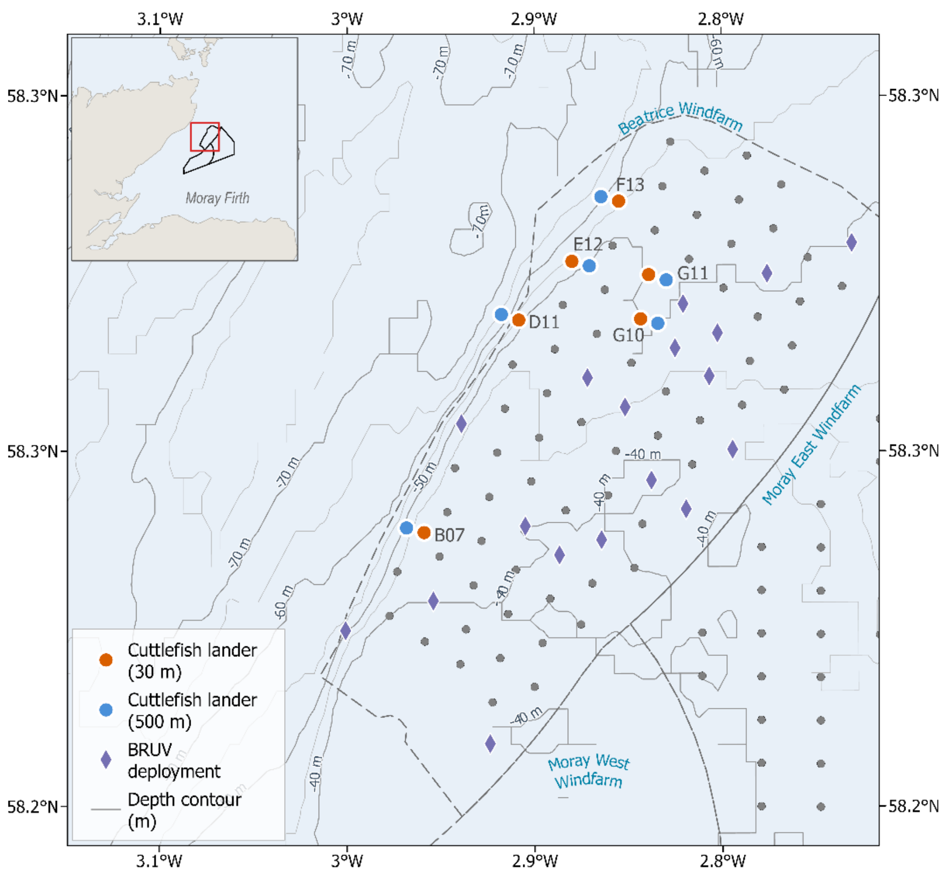

Figure 1. Location of Cuttlefish lander and BRUV deployments at the Beatrice Offshore Wind Farm, Moray Firth, Scotland, July 2024. Sampled turbine foundations are labelled. A BRUV deployment was also conducted at each Cuttlefish turbine location (n = 6); additional BRUV-only stations are shown as diamonds. Depth contours are shown at 10 m intervals. Inset: study area location within the Moray Firth.

2.2 Cuttlefish landers

The "Cuttlefish" lander are underwater stereo frames, which housed two Sony IMX662 cameras with 1080p resolution and recording at 30 frames per second. These landers were developed through a collaboration between the University of Exeter and Inkfish (formerly Arctic Rays), a US-based company (Fig. 2). The systems are ropeless to avoid entanglement with artificial structures during extended deployments. The systems are equipped with sacrificial weights to ensure they are negatively buoyant for deployment to the seabed. For retrieval, an acoustic release is used to jettison the sacrificial weights, at which point the system rises to the sea surface and is collected by a surface vessel. A marine licence was obtained permitting the deposition of the sacrificial weights (licence ref# 00010773). These weights are manufactured from mild steel that corrodes in the seawater.

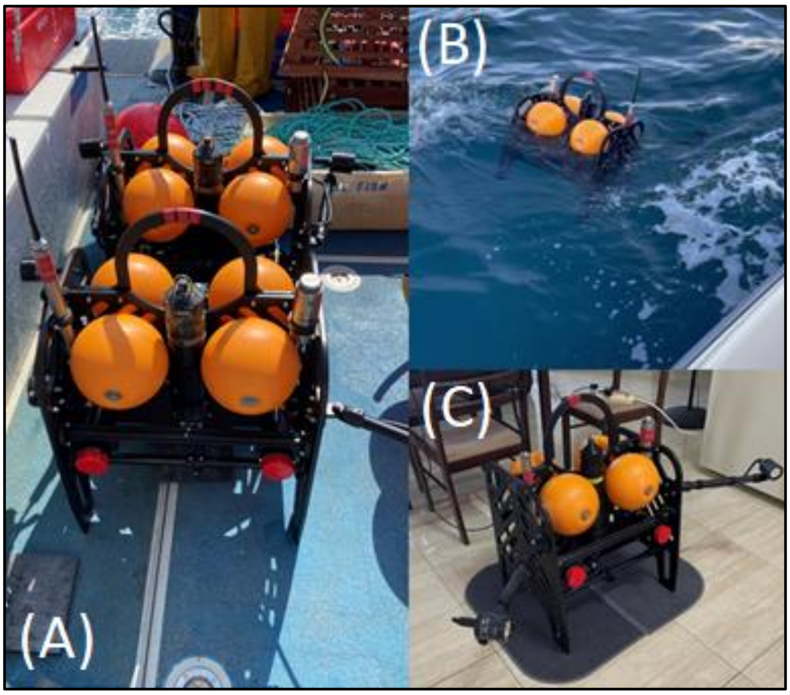

Figure 2. Cuttlefish lander system. (A) Landers prepared on deck, (B) lander floating at surface, (C) lander with light booms deployed

Each lander was equipped with two Inkfish LED lights (5,700 K colour temperature; 100° beam angle) and deployed at 25% output, providing a combined 3,000 lumens light intensity. The Cuttlefish systems have a battery life of approximately 48 hours when recording continuously, with programmable recording intervals available to extend deployment duration, with both white and red LED lighting options.

The systems use a stereo camera configuration enabling body length measurements. VHF and satellite tracking beacons are fitted in case of unexpected surfacing, and the systems have a maximum operational depth of 300 m. Each lander carried a temperature and pressure sensor, with recording at one-second intervals.

2.3 Sampling design

2.3.1 Cuttlefish landers

A paired sampling design was used to examine the influence of turbine proximity on marine species assemblages and abundance across diel periods. Each paired deployment consisted of a Cuttlefish lander positioned at either 30 m (near-field) from a turbine jacket foundation, representing the closest safe distance to assess direct turbine influence, and 500 m from the same turbine (far-field). The 500 m distance was selected to represent conditions away from the influence of the turbine structure.

Initial sites were chosen on the northwest side of the Beatrice wind farm due to their proximity to Wick (the home port for this research activity), which would enable easier handling of premature release of landers from the seabed, should they occur. Deployments were expanded to sites further east and south into the wind farm. In total, 12 Cuttlefish deployments (6 paired sets) were completed across 6 turbine locations during the 7-day survey period (Fig. 1; Table 1).

Cuttlefish landers were configured to record continuously using white lights at 25% intensity, with no bait. Paired deployments were conducted in close succession, with the 30 m unit deployed first. Landers were positioned approximately perpendicular to the prevailing bottom current direction, in either a WNW or ESE bearing depending on tidal state at the time of deployment (Fig. 3). Landers were deployed during daylight and retrieved the following morning.

2.3.2 Baited cameras

Cuttlefish deployment locations coincided with turbines where BRUV systems were deployed as part of a concurrent survey (Bicknell et al., 2026). This approach enabled subsequent comparison between baited and unbaited camera systems (2.7). BRUVs were Blue Abacus systems (Blue Abacus, https://www.blueabacus.org/) using two Go-Pro Hero cameras in stereo-recording configuration. Each BRUV was fitted with two high-output wide-angle LED video lights. At four of the six turbines, BRUV deployments preceded Cuttlefish lander deployments by 6 to 9 days. At one turbine (G10) both systems were deployed on the same day, and at one turbine (D11) the Cuttlefish deployment preceded the BRUV by one day. Given the small bait mass used (100 g) and the strong tidal flushing at the site, carry-over effects were not anticipated.

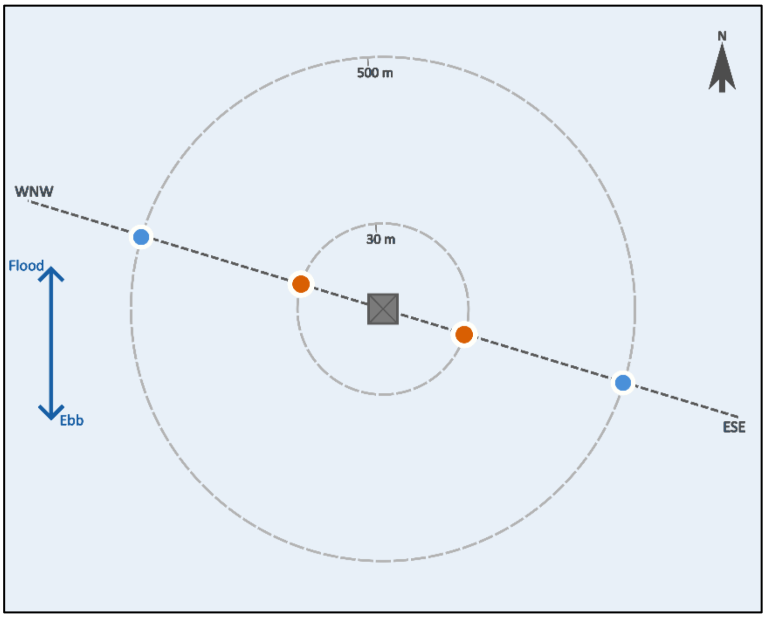

Figure 3. Cuttlefish lander deployment design at offshore wind turbine jacket foundations. Landers were deployed as a single pair: one at 30 m (orange circles) and one at 500 m (green circles) from the turbine foundation (grey square) along either a WNW or ESE bearing, approximately perpendicular to the prevailing tidal current direction (blue arrows). Dashed circles indicate distance from the turbine foundation. Deployment direction was determined by tidal state, with the 500 m unit positioned in a direct line from the turbine through the 30 m location.

Table 1. Summary of Cuttlefish deployments (times in UTC). †Cumulative of data gathered.

Deployment date	Tur-bine	Distance (m)	Direction (cardinal)	Latitude (WGS84)	Longitude (WGS84)	Retrieval date	†Data volume (GB)
19/07/2024 12:20	D11	30	WNW	58.280807	-2.92365	20/07/2024 11:20	79.0
19/07/2024 12:34	D11	500	WNW	58.282106	-2.931417	20/07/2024 11:09	78.7
21/07/2024 11:21	G11	30	ESE	58.291407	-2.865791	22/07/2024 10:15	79.9
21/07/2024 11:32	G11	500	ESE	58.290179	-2.857954	22/07/2024 10:25	78.7
22/07/2024 13:58	G10	30	ESE	58.281057	-2.869379	23/07/2024 10:03	69.7
22/07/2024 14:01	G10	500	ESE	58.279999	-2.861799	23/07/2024 10:14	49.4
23/07/2024 14:50	E12	30	ESE	58.294536	-2.899959	24/07/2024 10:34	69.1
23/07/2024 15:00	E12	500	ESE	58.293505	-2.892205	24/07/2024 11:15	56.1
24/07/2024 15:32	F13	30	WNW	58.308635	-2.879095	25/07/2024 14:18	78.3
24/07/2024 15:37	F13	500	WNW	58.30971	-2.887004	25/07/2024 13:50	79.7
25/07/2024 17:09	B07	30	ESE	58.232048	-2.973579	26/07/2024 7:40	50.3
25/07/2024 17:05	B07	500	ESE	58.230958	-2.965783	26/07/2024 8:10	52.7

2.4 Video processing and species identification

All video data were analysed using EventMeasure (www.seagis.com.au) and custom-developed YOLOv8 computer vision detection models (Lambrette et al., In prep.). Two measures of relative abundance were derived. The primary measure was mean count, the number of individuals detected per frame (at 1 frame per second) by the automated model across the full continuous recording. Mean count is an index of relative abundance and does not estimate the number of distinct individuals present. Mean count was preferred over MaxN as the abundance measure from automated detection data as this measure integrates across all frames and provides a stable estimate of abundance. For validation, and for comparison with the concurrent BRUV survey, MaxN was also quantified in lander data using manual annotation.

Distinguishing between species using horizontal video can be challenging in the marine environment, particularly for flatfish. Common dab *Limanda limanda* and European flounder *Platichthys flesus* were therefore grouped at taxonomic order level as Pleuronectiformes spp. for all analyses, while European plaice *Pleuronectes platessa*, which are sufficiently distinct for reliable identification, were recorded separately and excluded from the flatfish group. Although the automated model detected at family level (Gadidae and Pleuronectiformes), analyses are reported as haddock and flatfish, reflecting that these families were overwhelmingly represented by haddock *Melanogrammus aeglefinus*, and by common dab and European flounder, respectively, at this site. These taxa dominated fish observations across all datasets, consistently accounting for over 94% of total fish abundance in the BRUV 30-minute deployments, over 86% in the initial 30 minutes of the Cuttlefish lander deployments, and 93% in the manually annotated Cuttlefish two-minute hourly samples.

2.4.1 Automated detection

Automated detection was performed using a YOLO-based object detection model adapted from the YOLO-BRUV model developed for baited remote underwater video within the wider project (Bicknell et al., 2026; Lambrette et al., 2026). As the original YOLO-BRUV model performed poorly when applied directly to the Cuttlefish lander video, which differs in lighting, camera configuration and field of view, the model was retrained for the Cuttlefish system. A library of 500 training images was created by annotating all organisms in the frames at the zero-minute and one-minute elapsed interval for every hour of video data. This process reflected the same annotation protocol as the original model development for BRUVs. The retrained model was applied to the complete video record of all twelve deployments, sampling the first frame of every second (1 fps) and returning the number of individuals of each focal taxon group detected in each sampled frame, with mean count derived across the full continuous recording. Detections were made at family level (Gadidae and Pleuronectiformes) and for validation were compared against manual annotation of the same frames at the same taxonomic resolution) (2.7). Only detections with a confidence score of at least 0.6 were retained for abundance estimation.

2.4.2 Manual analysis (human annotator)

Cuttlefish landers recorded continuously throughout each deployment, and two subsets of resulting video data were annotated manually by a single trained observer to ensure consistency. For direct comparison with the concurrent BRUV survey, the initial 30 minutes of each Cuttlefish deployment were analysed following the standard BRUV observation protocol (2.8). Analysis began once the camera system had settled on the seabed and continued for 30 subsequent minutes (Bicknell et al., 2026), with all individuals identified to the lowest possible taxonomic level. Separately, to characterise diel variation in abundance throughout the extended Cuttlefish recordings, the first two minutes of every hour were annotated across the full deployment duration (2.7).

2.4.3 Scene contamination

Video data gathered at approximately 50 m depth during daylight hours exhibited variable levels of contamination by infrared light from solar radiation penetrating to the seabed. The Cuttlefish cameras were developed to operate in low-light environments using white or red illumination and were not fitted with infrared cut filters, rendering them susceptible to solar infrared interference under bright conditions. To quantify the impact of this contamination on image quality across the survey, a subjective red light contamination score (1 to 4) was assigned to each two-minute observation window analysed (one per hour of deployment; 2.7), based on the first 10 seconds of that window. A score of 1 indicated minimal or no visible red contamination, 2 limited contamination, 3 moderate contamination, and 4 heavy contamination affecting visibility across much of the field of view. Scoring was conducted by a single observer concurrently with MaxN annotation.

The video processing activities and their associated abundance measures, sampling schemes and processing tools, are summarised in Table 2.

Table 2. Video processing activities.

Purpose	Measure	Unit	Sampling	BRUV (Human)	Cuttlefish (Human)	Cuttlefish (YOLO)
Automated detection	Mean count	Mean individual per frame	1 fps, full recording	-	-	✓
Validation	MaxN	Max individuals in a frame	First 2 minutes of every hour	-	✓	-
Baited versus unbaited	MaxN	Max individuals in a frame	First 30 minutes	✓	✓	-
Scene contamination	Red light score	1-4 ordinal scale	First 10 seconds of every hour	-	✓	-

2.5 Environmental data

Seabed current speed data were obtained from POLPRED CS20 sigma 1 tidal prediction models (National Oceanography Centre; https://noc-innovations.com/services/tide-prediction-software/offshore-software/) for the coordinates (WGS84) of each deployment location. POLPRED provides harmonic tidal predictions of current speed (m/s) and direction (degrees) at the seabed, which were extracted at hourly resolution for the duration of each deployment. Current speed was matched to each observation by date and hour and included as a continuous covariate in statistical modelling. Current speed values were standardised prior to modelling.

2.6 Diel patterns in fish abundance

Diel patterns in fish abundance were characterised from the automated detections across the full duration of each deployment. For each deployment hour, the mean count was calculated, separately for Gadidae and Pleuronectiformes (hereafter mean count). Hours in which a taxon was not detected were assigned a mean count of zero. Whereas MaxN records only the single most populated frame and so reflects peak abundance, the mean count averages detections across all frames and so reflects abundance integrated over the full recording. Manual annotation is necessarily limited to MaxN, whereas automated frame-by-frame detection permits this continuous measure throughout each deployment.

Each deployment-hour was classified into one of four diel periods (dawn, day, dusk, or night). Civil twilight times (sun angle -6° below horizon) were calculated using the suncalc R package for each deployment date at the site coordinates (Thieurmel & Elmarhraoui, 2022). Dawn was defined as the period from the start of civil twilight to sunrise (mean period 04:25-05:32), day from sunrise to sunset (05:32-21:35), dusk from sunset to the end of civil twilight (21:35-22:42), and night from the end of civil twilight to the start of civil twilight the following morning (22:42-04:25).

Generalised linear mixed models (GLMMs) with a Tweedie error distribution were fitted to mean count for each taxon, with distance (30 m, 500 m), diel period (dawn, day, dusk, night) and their interaction as fixed effects. A Tweedie distribution was selected as appropriate for a continuous, non-negative response containing exact zeros (Foster & Bravington, 2013). Turbine was included as a random intercept to account for the paired sampling design, with both distance treatments nested within each turbine. Deployment was not used as the random effect because the paired design means distance is a within-turbine factor; grouping by deployment would confound distance with the random effect. Seabed current speed was evaluated as an additional covariate, both as a main effect and interacting with distance, but did not improve model fit for either taxon and was excluded from the final models. All models were fitted using glmmTMB (Brooks et al., 2017). Final model structure for both taxa was:

$$\textit{Mean count} \sim \textit{Distance} \times \textit{Diel Period} + (1 \mid \textit{Turbine})$$

Statistical significance of fixed effects was assessed using Type II Wald chi-square tests. Distance effects within each diel period were estimated as ratios of estimated marginal means (30 m / 500 m) with 95% confidence intervals on the response scale, computed using the emmeans package (Lenth & Piaskowski, 2025). All analyses were conducted in R version 4.2.1. (R Team, 2022).

2.7 Validation of automated analysis

To validate the automated abundance estimates, the diel and distance patterns recovered by the model were compared against an independent manual analysis of a subset of the video data. To characterise temporal patterns in fish abundance throughout the multi-hour deployment periods, the first two minutes of every hour from each Cuttlefish deployment were analysed manually.

This hourly sampling provided 15-23 observation periods per deployment (mean ± SD: 20.5 ± 2.8 hours) and generated 236 total observation periods across the 12 deployments. A two-minute sampling window was used to balance comprehensive temporal coverage with manageable processing requirements while providing sufficient observation time for MaxN quantification. Relative abundance was quantified as MaxN, and observation periods in which a focal species was not detected were assigned a MaxN of zero. Diel periods were assigned as described in 2.6.

Generalised linear mixed models with a negative binomial error distribution were fitted to MaxN for gadoid and Pleuronectiformes, with the same fixed-effect and random-effect structure as the abundance analysis (distance, diel period and their interaction, with turbine as a random intercept). A negative binomial distribution was selected over Poisson due to overdispersion in the count data, as confirmed through dispersion tests. Seabed current speed did not improve model fit ($\Delta AIC < 2$ in all comparisons) and was excluded. All models were fitted using glmer.nb in lme4 (Bates et al., 2015). The final model structure for both species was:

$$MaxN \sim Distance \times Diel\ Period + (1 \mid Turbine)$$

Significance and distance ratios were obtained as in 2.6. Agreement between the automated and manual analyses was assessed by comparing the direction and magnitude of the distance and diel effects recovered by each.

2.8 Comparison of baited and unbaited camera systems

To compare MaxN between baited and unbaited camera systems, the initial 30 minutes of each Cuttlefish deployment were analysed alongside the full 30-minute BRUV deployments conducted at the same turbine locations during the survey period (Bicknell et al., 2026). BRUV deployments were conducted at 30 m and 240 m from turbine foundations, while Cuttlefish deployments were at 30 m and 500 m. As the far-field distances differ between camera types (240 m vs 500 m), a direct comparison at this distance would confound camera type with distance from turbine. The analysis was therefore restricted to the 30 m deployments only, where both camera systems sampled at the same distance from the turbine foundation. This provided 30 deployments in total: 24 BRUV and 6 Cuttlefish. For this analysis, comparisons did not use computer vision techniques and were entirely based on human annotation.

GLMMs were fitted to MaxN data for each species, with camera type (BRUV vs Cuttlefish) and standardised current speed as fixed effects and turbine identity as a random intercept. Model selection compared Poisson and negative binomial distributions crossed with turbine and deployment as random effects (four candidate models per species). For both haddock and flatfish, Poisson models with turbine as the random effect were selected based on AIC, with no evidence of overdispersion (dispersion ratios of 0.64 and 0.56 respectively). The final model structure for both species was:

$$MaxN \sim Camera\ Type + Current\ Speed + (1 \mid Turbine)$$

Statistical significance was assessed using Type II Wald chi-square tests via the car package. Estimated marginal means and pairwise ratios (BRUV / Cuttlefish) were computed using emmeans (Lenth & Piaskowski, 2025).

3. Results

3.1 Survey summary

Cuttlefish lander deployments (n = 12) were successfully completed at six turbine foundations within the Beatrice Offshore Wind Farm between 19 and 26 July 2024 (Table 1). At each turbine, paired deployments were conducted at 30 m and 500 m from the jacket foundation. These deployments generated 246 hours of cumulative stereo video data (821.6 GB), with a mean ± SD of 68.5 ± 12.1 GB per deployment. Mean deployment duration was 20.5 ± 2.8 hours (range 14.5–23.2 hours). Mean deployment depth was 52.3 ± 5.2 m (range 43–62 m). Mean seabed water temperature, calculated as the grand mean of individual deployment means, was 11.5 °C (SD = 0.18°C, n = 10 deployments; onboard temperature sensor from the D11 paired deployment were not recovered). All deployments were classified as fine sediment habitat.

All acoustic release recovery operations were successful. Of the 12 recoveries, seven (58%) released on the first command; the remaining five required between two and six commands to initiate release.

Representative imagery from the deployments illustrates the range of taxa observed in the vicinity of the turbine jacket foundations (Fig. 4), including haddock and common dab, the most frequently recorded species. Five observations of critically endangered flapper skate (*Dipturus intermedius*) were recorded across the survey period.

3.2 Environmental data

Current speeds were broadly similar across the six turbine locations, with deployment means ranging from 0.15 m/s at D11 to 0.22 m/s at E12. Peak current speeds increased from 0.25 m/s during the earlier deployments (19–20 July) to 0.36 m/s during the later deployments (23–25 July), reflecting the transition from neap to spring tides over the survey period. Individual Cuttlefish deployments spanned between 1.2 and 1.9 tidal cycles depending on deployment duration. The concurrent BRUV survey operated 15–24 July, with the earlier BRUV deployments (15–17 July) coinciding with neap tides and weaker current speeds (mean 0.09 m/s) than those experienced during the Cuttlefish survey period (Fig. 5).

Figure 4a. Haddock (*Melanogrammus aeglefinus*), common dab (*Limanda limanda*) at turbine G10.t

Figure 4b. Male flapper skate (*Dipturus intermedius*) at turbine E12.

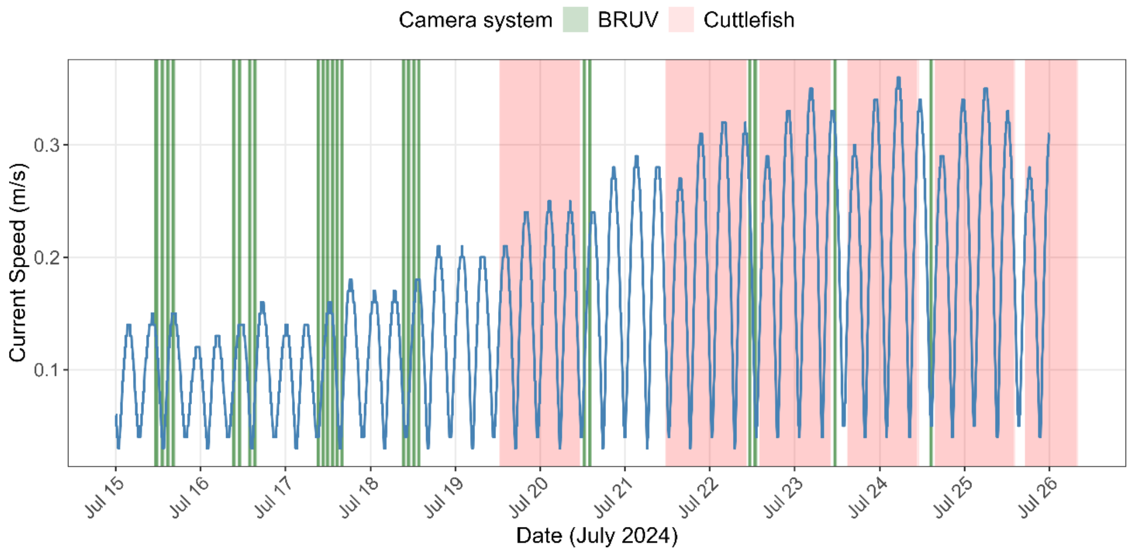

Figure 5. Predicted bottom current speed (m/s) at the Beatrice Offshore Wind Farm (15–26 July 2024), derived from POLPRED CS20 tidal predictions at the farm centroid (58.281°N, 2.901°W) at 15-minute resolution. Shaded regions indicate deployment periods for Cuttlefish landers (pink) and BRUVs (green).

Table 3. Species recorded across 236 two-minute observation windows from 12 Cuttlefish lander deployments at the Beatrice Offshore Wind Farm, July 2024. Total MaxN is the sum of maximum counts across all observation windows in which a species was recorded.

Common name	Scientific name	Family	No. Observations	Total MaxN
Flatfish	*Pleuronectiformes spp*	Pleuronectidae	221	2,857
Haddock	*Melanogrammus aeglefinus*	Gadidae	160	1,393
European Plaice	*Pleuronectes platessa*	Pleuronectidae	84	132
Common Hermit Crab	*Pagurus bernhardus*	Paguridae	39	57
Poor Cod	*Trisopterus minutus*	Gadidae	14	52
Whiting	*Merlangius merlangus*	Gadidae	29	38
Grey Gurnard	*Eutrigla gurnardus*	Triglidae	8	10
Common Starfish	*Asterias rubens*	Asteriidae	8	8
Norway Pout	*Trisopterus esmarki*	Gadidae	4	8
Sand Star	*Astropecten irregularis*	Astropectinidae	5	5
Flapper Skate	*Dipturus intermedius*	Rajidae	5	5
Dragonet	*Callionymus lyra*	Callionymidae	5	5
Common Whelk	*Buccinum undatum*	Buccinidae	3	3
Ophiuroid	*Ophiura albida*	Ophiuridae	2	2
European Squid	*Loligo vulgaris*	Loliginidae	1	1

3.3 Diel patterns in fish abundance

3.3.1 Species richness and abundance

A total of 15 taxa from 10 families were recorded across the Cuttlefish deployments (Table 3; previous page); these were determined from the 2-minute human annotated observations. Flatfish (*Pleuronectiformes* spp.) and haddock (*Melanogrammus aeglefinus*) together accounted for 93% of all individuals recorded (combined summed MaxN = 4,250 of 4,576 total), consistent with the >90% dominance of these two groups reported from concurrent BRUV surveys at the same site (Bicknell et al., 2026).

3.3.2 Temporal coverage and sampling effort

The automated model was applied to the continuous recordings of all twelve deployments, providing 253 deployment-hours of video data across the four diel periods. Reflecting the natural duration of each period at 58°N in July, most hours were daytime (n = 169, 66.8%) then night (n = 60, 23.7%), with fewer at dawn (n = 12, 4.7%) and dusk (n = 12, 4.7%). All deployments spanned at least one transition between day and night, ensuring that each diel period was sampled across multiple turbines.

3.3.3 Validating novel abundance metrics

Mean count per hour is an abundance metric not commonly encountered in marine video imagery studies, where MaxN predominates, and is made possible here by the continuous recording of the Cuttlefish landers and the per-frame output of the computer vision model. To relate this measure to more frequently used MaxN, the two metrics were compared hourly across all deployments (Fig. 6). Mean count was positively correlated with MaxN for Gadidae (Spearman's $\rho = 0.96$) and Pleuronectiformes ($\rho = 0.98$), confirming that the two metrics capture the same underlying variation in abundance, while remaining distinct measures: MaxN reflects peak abundance in a single frame; whereas mean count integrates abundance across the full hour.

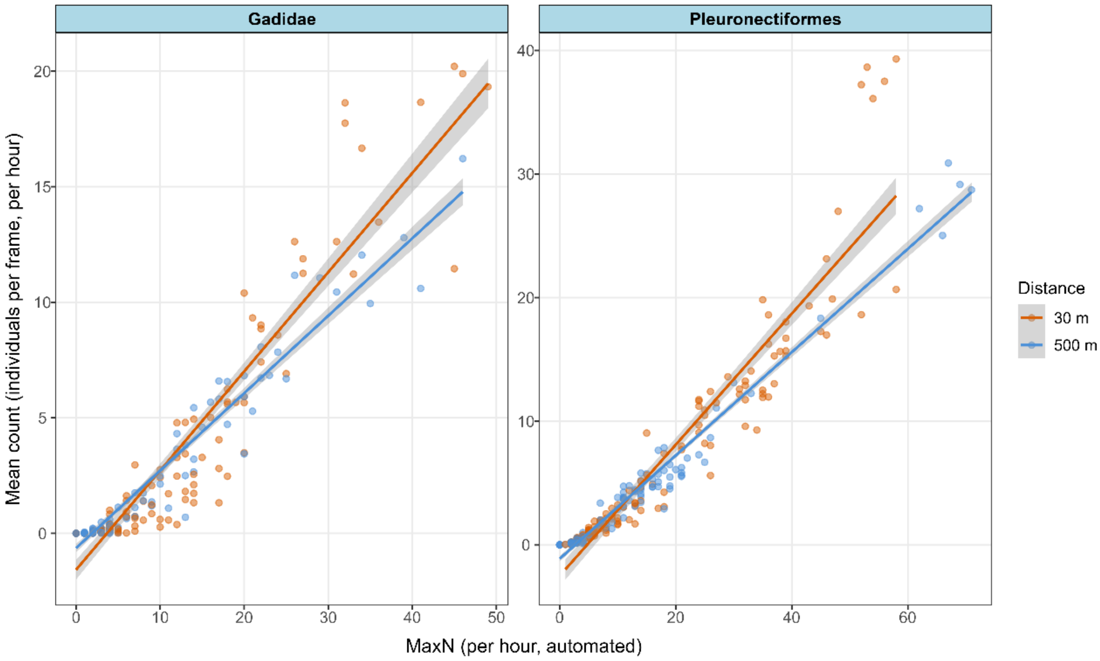

Figure 6. Relationship between automated MaxN and automated mean count, computed per hour from the machine learning detections, for Gadidae (left) and Pleuronectiformes (right). Each point represents one deployment-hour; orange points are deployments at 30 m and blue points at 500 m from turbine foundations. Lines show linear fits with 95% confidence intervals (shaded). Mean count is the average number of individuals detected per frame across the hour; MaxN is the maximum number detected in any single frame within the hour.

3.3.4 Gadidae

Sampled frames by the automated detector identified Gadidae 41.1% of frames, with detections more frequent at 30 m (48.3% of frames) than at 500 m (33.9%). Mean count across deployments ranged from 0.24 to 6.36 individuals per frame and was higher at 30 m (3.32 per frame) than at 500 m (1.90). Detections were skewed among turbines, with G11 (38%) and G10 (27%) together accounting for 65% of all Gadidae recorded. Gadidae displayed a strong diel pattern at both distances, with low abundance during daytime, a sharp increase around dusk, and peak values during the night that persisted through dawn before declining after sunrise (Fig. 7). This pattern was broadly consistent across all six turbines, although its degree varied considerably between them (Fig. S1).

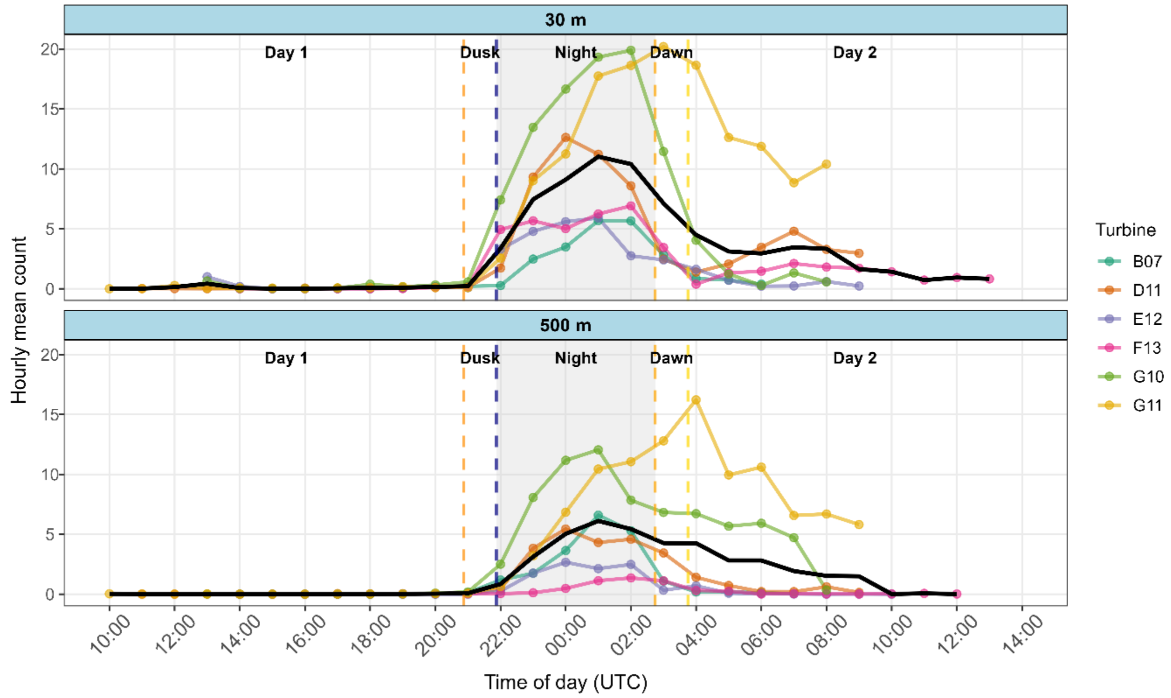

Figure 7. Gadidae hourly mean count over time of day at 30 m (upper panel) and 500 m (lower panel) from turbine foundations. Individual turbines are shown as coloured lines; the bold black line shows the grand mean across all turbines. Dashed vertical lines indicate the mean timing of dusk (orange), midnight (blue) and dawn (yellow).

Diel period was the strongest predictor of Gadidae mean count ($\chi^2 = 269.2$, df = 3, $p < 0.001$), followed by distance from the turbine foundation ($\chi^2 = 32.9$, df = 1, $p < 0.001$; Table 4), with abundance averaging 2.3 times higher at 30 m than 500 m across the diel cycle (95% CI 1.47–3.60). The Distance × Diel Period interaction was not significant ($\chi^2 = 0.3$, df = 3, $p = 0.965$), indicating that the effect of proximity to turbines was consistent across all four diel periods. Predicted mean count was highest during dawn and night at both distances (Fig. 8).

Table 4. Type II Wald chi-square tests for the selected Gadidae and Pleuronectiformes mean-count GLMMs. Significance: *** $p < 0.001$, ** $p < 0.01$, * $p < 0.05$, ns = not significant. Significant terms are in bold.

Species	Effect	χ^2	df	p	
Gadidae	**Distance**	**32.9**	**1**	**<0.001**	***
Gadidae	**Diel Period**	**269.2**	**3**	**<0.001**	***
Gadidae	Distance × Diel Period	0.3	3	0.965	ns
Pleuronectiformes	**Distance**	**53.6**	**1**	**<0.001**	***
Pleuronectiformes	**Diel Period**	**67.2**	**3**	**<0.001**	***
Pleuronectiformes	Distance × Diel Period	5.3	3	0.149	ns

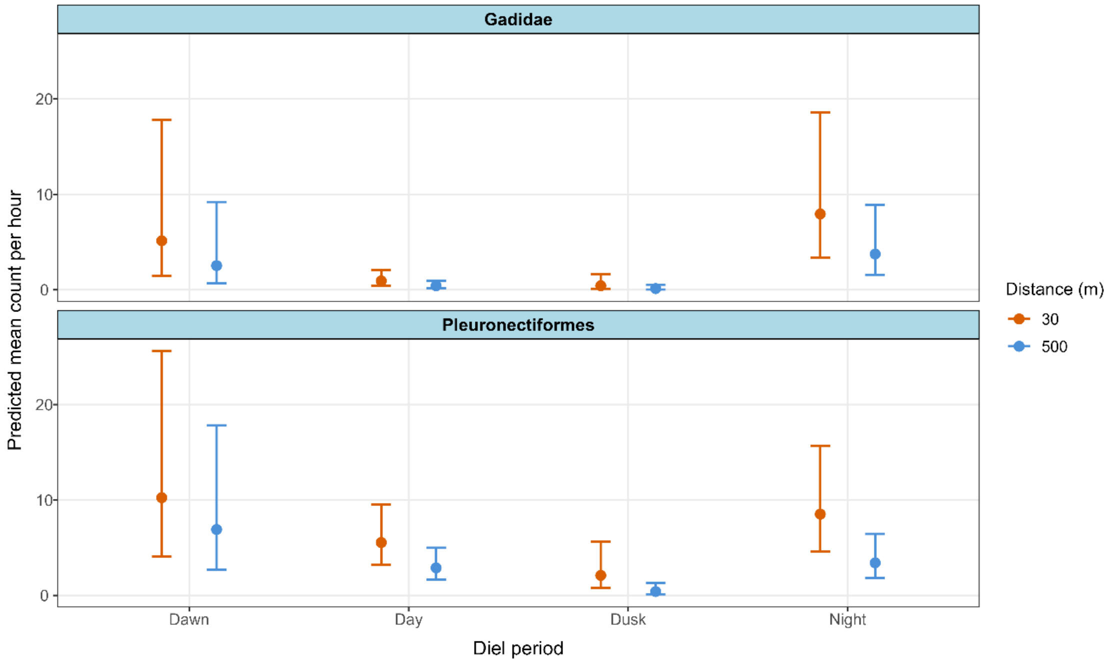

Figure 8. Predicted mean count (± 95% confidence intervals) from the selected Tweedie GLMMs for Gadidae (upper panel) and Pleuronectiformes (lower panel) by diel period and distance from turbine foundation.

At 30 m, predicted mean count was 8.0 at night (95% CI 3.4–18.6) and 5.1 at dawn (1.5–17.8), declining to 0.9 during the day (0.4–2.06) and 0.4 at dusk (0.1–1.6). The same diel pattern was evident at 500 m but at lower abundance throughout (night: 3.8, 1.7–8.9; dawn: 2.5, 0.7–9.2; day: 0.4, 0.2–0.95; dusk: 0.1, 0.03–0.5). Gadidae mean count was significantly higher at 30 m than 500 m during the day (ratio 2.2, $p < 0.001$) and night (2.1, $p = 0.001$), with a similar but non-significant trend at dusk (3.0, $p = 0.099$) and dawn (2.00, $p = 0.193$; Table 5).

Table 5. Pairwise distance effect ratios (30 m / 500 m) by diel period for Gadidae and Pleuronectiformes. Ratios greater than 1 indicate higher abundance at 30 m. Estimated from marginal means of the selected mean-count GLMM for each taxon. Significance: *** $p < 0.001$, ** $p < 0.01$, * $p < 0.05$, $p < 0.1$, ns = not significant.

Species	Diel period	Ratio (30 m / 500 m)	95% CI	z	p	
Gadidae	Dawn	2.00	0.70 – 5.71	1.30	0.193	ns
Gadidae	**Day**	**2.17**	**1.54 – 3.07**	**4.37**	**<0.001**	***
Gadidae	Dusk	3.03	0.81 – 11.26	1.65	0.099	.
Gadidae	**Night**	**2.14**	**1.35 – 3.39**	**3.24**	**0.001**	**
Pleuronectiformes	Dawn	1.47	0.66 – 3.25	0.95	0.341	ns
Pleuronectiformes	**Day**	**1.86**	**1.47 – 2.36**	**5.15**	**<0.001**	***
Pleuronectiformes	**Dusk**	**5.04**	**1.78 – 14.24**	**3.05**	**0.002**	**
Pleuronectiformes	**Night**	**2.52**	**1.72 – 3.69**	**4.78**	**<0.001**	***

3.3.5 Pleuronectiformes

Pleuronectiformes were more ubiquitous than Gadidae, detected in 69.6% of all sampled frames and at consistently higher densities, with detections more frequent at 30 m (78.7% of frames) than at 500 m (60.5%). Mean count across deployments ranged from 1.5 to 14 individuals per frame and was higher at 30 m (7.4 per frame) than at 500 m (3.8). Detections were heavily skewed among turbines, with D11 alone accounting for 38% of all Pleuronectiformes recorded, followed by F13 (18%) and E12 (17%). Pleuronectiformes were present at low levels during daytime at both distances, with a step-change increase around dusk that was maintained through the night and into dawn, a pattern evident across all six turbines despite marked differences in abundance (Fig. 9 and Fig. S2).

Distance from the turbine foundation was highly significant ($\chi^2 = 53.6$, df = 1, $p < 0.001$), as was diel period ($\chi^2 = 67.2$, df = 3, $p < 0.001$; Table 4 As for Gadidae, the Distance × Diel Period interaction was not significant ($\chi^2 = 5.33$, df = 3, $p = 0.149$); the aggregation effect was therefore consistent across the diel cycle, with abundance averaging 2.43 times higher at 30 m than 500 m overall (95% CI 1.72–3.44).

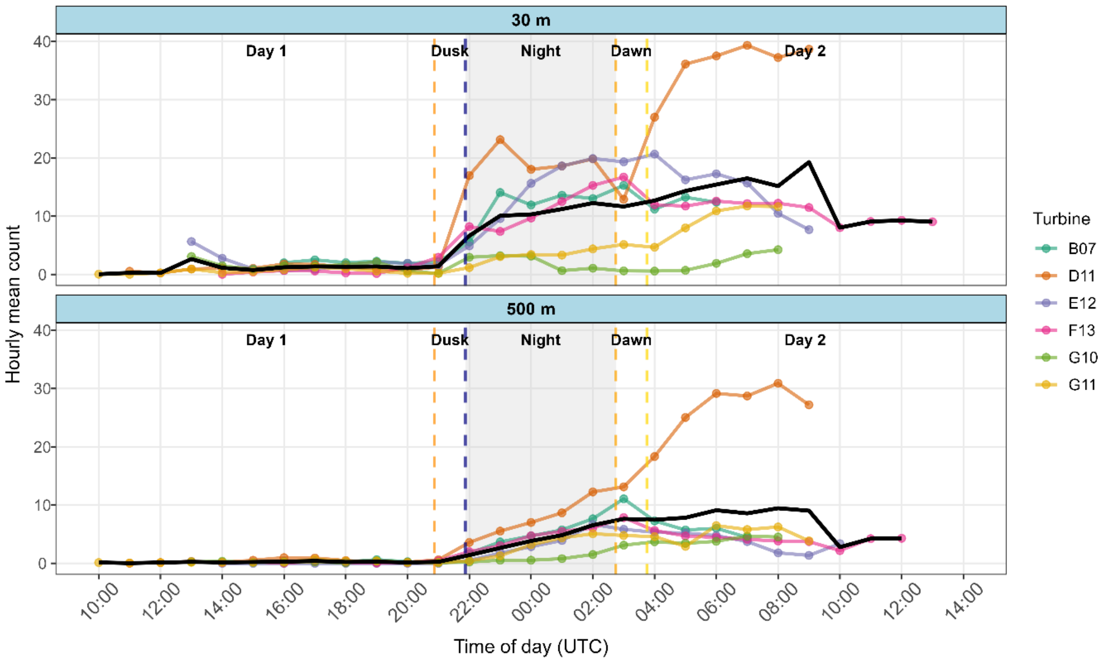

Figure 9. Pleuronectiformes hourly mean count over time of day at 30 m (upper panel) and 500 m (lower panel) from turbine foundations. Individual turbines are shown as coloured lines; the bold black line shows the grand mean across all turbines. Dashed vertical lines and shading as in Figure 7.

Predicted mean count at 30 m was highest at dawn (10.2, 95% CI 4.1–25.6) and night (8.5, 4.6–15.7), with daytime values remaining relatively elevated (5.5, 3.2–9.5) compared to a marked dip at dusk (2.1, 0.8–5.6). At 500 m, abundance followed a similar diel pattern but at consistently lower levels (dawn: 6.9, 2.7–17.8; night: 3.4, 1.8–6.5; day: 2.9, 1.7–5.0; dusk: 0.4, 0.1–1.3; Fig. 8). Pleuronectiformes mean count was significantly higher at 30 m than 500 m during the day (ratio 1.86, $p < 0.001$), dusk (5.0, $p = 0.002$) and night (2.5, $p < 0.001$), with a similar but non-significant trend at dawn (1.5, $p = 0.341$; Table 5).

3.4 Comparison with automated analysis

The manual analysis sampled the first two minutes of every hour across all twelve deployments, yielding 236 two-minute observation periods. As with the automated analysis, most observation periods fell within daytime (n = 155, 65.7%) and night (n = 57, 24.2%), with fewer at dawn (n = 12, 5.1%) and dusk (n = 12, 5.1%). Each period provided a single MaxN per deployment-hour, in contrast to the continuous frame-by-frame mean count used in the automated analysis. The two analyses also differ in taxonomic resolution: the automated model detects to family, whereas the manual annotator identified haddock to species. The gadid comparison is therefore between automated Gadidae detections and manual haddock counts, though as haddock made up 93% of all gadids recorded (Table 3) the two correspond closely; the flatfish comparison is at order level (Pleuronectiformes) in both methods.

The manual analysis recovered the same spatial and temporal patterns as the automated model for both taxa. Abundance was significantly higher at 30 m than 500 m (haddock $\chi^2 = 22.1$, df = 1, $p < 0.001$; flatfish $\chi^2 = 23.2$, df = 1, $p < 0.001$) and varied strongly with diel period (haddock $\chi^2 = 134.4$, df = 3, $p < 0.001$; flatfish $\chi^2 = 21.3$, df = 3, $p < 0.001$), with peak abundance during the night and into dawn. As in the automated analysis, the Distance × Diel Period interaction was not significant (haddock $\chi^2 = 0.58$, df = 3, $p = 0.900$; flatfish $\chi^2 = 2.81$, df = 3, $p = 0.422$).

The magnitude of the distance effect was also comparable between the two analyses (Table 6). For both taxa, the direction and significance of the distance effect agreed across diel periods, with a significant reef effect during day and night, a non-significant trend at dawn, and a dusk effect that was significant for flatfish but not haddock.

Table 6. Distance effect ratios (30 m / 500 m) by diel period from the automated analysis (mean count) and the manual analysis (MaxN). Automated ratios are based on all Gadidae and Pleuronectiformes detections; manual ratios are based on haddock and flatfish. Ratios greater than 1 indicate higher abundance at 30 m. Significance: *** p < 0.001, ** p < 0.01, * p < 0.05, p < 0.1, ns = not significant.

Taxon	Diel period	Automated ratio	p	Manual ratio	p
Gadidae / haddock	Dawn	2.00	0.193 ns	1.50	0.342 ns
Gadidae / haddock	**Day**	**2.17**	**<0.001 *** **	**1.57**	**<0.001 *** **
Gadidae / haddock	Dusk	3.03	0.099 .	2.22	0.097 .
Gadidae / haddock	**Night**	**2.14**	**0.001 ** **	**1.71**	**0.007 ** **
Pleuronectiformes / flatfish	Dawn	1.47	0.341 ns	1.33	0.545 ns
Pleuronectiformes / flatfish	**Day**	**1.86**	**<0.001 *** **	**1.54**	**0.001 *** **
Pleuronectiformes / flatfish	**Dusk**	**5.04**	**0.002 ** **	**3.05**	**0.019 * **
Pleuronectiformes / flatfish	**Night**	**2.52**	**<0.001 *** **	**1.97**	**0.002 ** **

3.5 Comparison of baited and unbaited camera systems

To compare MaxN between baited (BRUV) and unbaited (Cuttlefish) census methods, analysis of video data was restricted to deployments at 30 m from turbine foundations, the distance common to both survey methods. This comparison yielded 30 paired observations across six turbines: 24 baited (30-minute baited BRUVs) and six unbaited (Cuttlefish first 30 minutes of unbaited continuous recording) deployments. This comparison only used data gathered during daylight hours, with BRUV deployments typically recorded between 10:00 and 15:00 UTC and the Cuttlefish 30-minute samples falling between 08:00 and 14:00 UTC.

Poisson GLMMs with turbine identity as a random intercept were fitted for each species, as overdispersion tests confirmed the Poisson distribution was appropriate for both haddock (dispersion ratio = 0.73, p = 0.83) and flatfish (dispersion ratio = 0.70, p = 0.87). Current speed was included as a covariate but was not significant for either species (haddock: $\chi^2 = 0.23$, p = 0.63; flatfish: $\chi^2 = 0.90$, p = 0.34).

Camera type was highly significant for both species (Table 7). For haddock, baited deployments using BRUVs detected approximately 4 times more individuals than unbaited deployments using Cuttlefish (predicted mean MaxN: BRUV = 10.1, 95% CI: 8.2–12.4; Cuttlefish = 2.5, 95% CI: 1.5–4.4; ratio = 3.96, p < 0.001). For flatfish, baited deployments detected approximately 2.6 times more individuals than unbaited deployments (predicted mean MaxN: BRUV = 17.0, 95% CI: 12.4–23.4; Cuttlefish = 6.6, 95% CI: 4.4–10.1; ratio = 2.56, p < 0.001; Table 7).

Table 7. Comparison of haddock and flatfish MaxN between BRUV and Cuttlefish camera systems at 30 m from turbine foundations. Predicted mean MaxN and BRUV / Cuttlefish ratios are estimated from Poisson GLMMs with turbine identity as a random intercept and current speed as a covariate. Significance: *** $p < 0.001$.

Species	Baited mean (95% CI)	Unbaited mean (95% CI)	Ratio (baited/ un-baited)	χ^2	p	
Haddock	10.1 (8.2–12.4)	2.5 (1.5–4.4)	3.96	25.9	<0.001	***
Flatfish	17.0 (12.4–23.4)	6.6 (4.4–10.1)	2.56	37.4	<0.001	***

3.6 Scene contamination

Red contamination scores were assigned to each of the 236 two-minute observation windows (Fig. 10), with example images illustrating each score category (Fig. 11). across all deployments, 55.8% of observation windows scored 1 (minimal or no contamination) and 25.4% scored 2, with the remaining 18.8% scoring 3 or 4 (median and mode = 1, n = 224; Fig. 10).

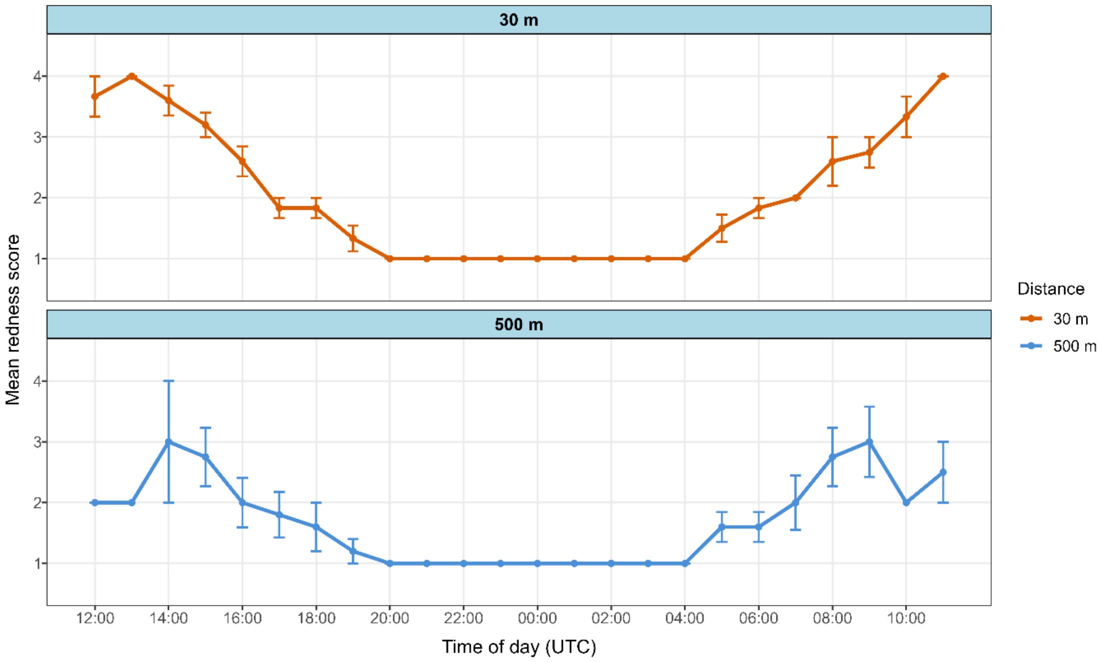

Figure 10. Mean hourly red contamination score at 30 m (orange) and 500 m (green) Cuttlefish deployments. Scores range from 1 (minimal or no red contamination) to 4 (heavy contamination). Error bars show standard error.

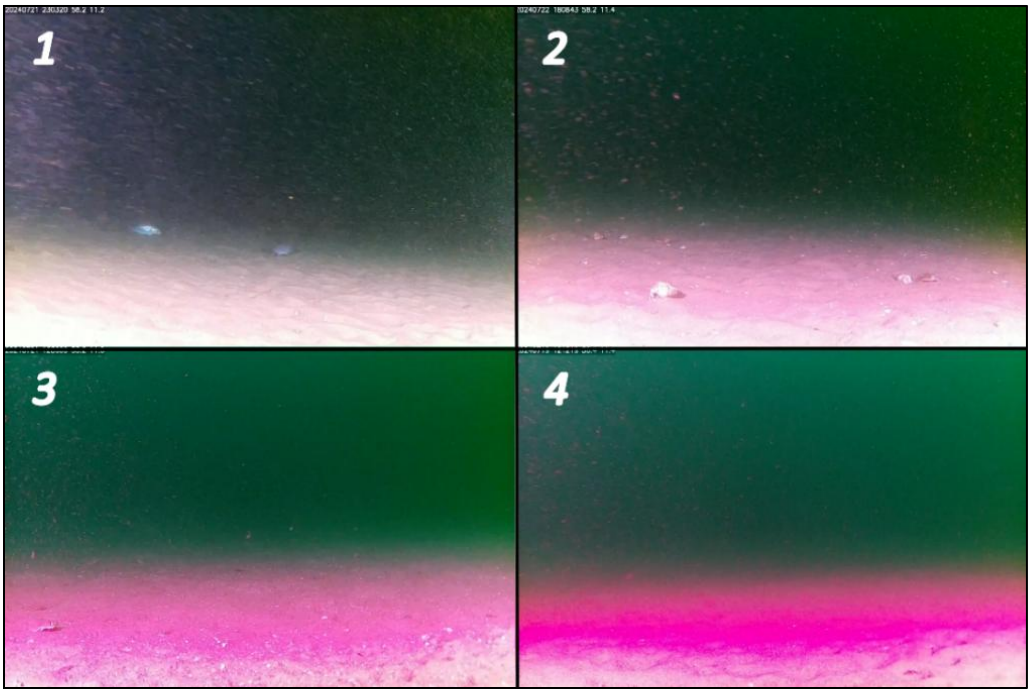

Figure 11. Representative lander images illustrating red contamination scores from 1 (minimal) to 4 (heavy).

Contamination was entirely absent between 20:00 and 04:00, when every window scored 1, reflecting the absence of solar infrared input during darkness. Scores increased from approximately 05:00 onwards, and between 08:00 and 15:00 no window was free of contamination, before declining through the evening to minimal levels by 20:00.

In the most heavily contaminated images (score 4), redness extended across the lower portion of the field of view making identification of individual fish in static frames more challenging, particularly for cryptically coloured flatfish resting on the seabed. However, when video data were viewed at standard play speed (30 fps), fish movement provided sufficient contrast for reliable identification and MaxN counting throughout the affected windows. Heavily contaminated images also coincided with daytime periods when fish abundance was lowest (3.3). As such, the practical impact on MaxN quantification across the dataset was limited.

4. Discussion

4.1 Effects of turbine distance on fish abundance

Both haddock and flatfish were significantly more abundant at 30 m from the turbine jacket foundations than at 500 m, consistent with the artificial reef effect documented at offshore wind farms across the North Sea (Degraer et al., 2020). This pattern concurs with results from the concurrent BRUV survey at the same site (Bicknell et al., 2026). The distance effect was of similar magnitude for the two taxa, with approximately twice the abundance at 30 m when compared with 500 m during the day and night (Table 5). For both taxa this pattern was consistent across all four diel periods, with the Distance × Diel Period interaction non-significant, indicating that the strength of the aggregation effect did not vary with time of day.

Abundance varied among turbine sites, with G11 and G10 (more towards the centre of the wind farm; Fig. 1) together accounting for 65% of all gadoids detected and D11 (on the periphery of the wind farm) alone responsible for 38% of all flatfish. This site-level variability is consistent with the concurrent BRUV survey, which reported significant turbine-level effects on both abundance and biomass (Bicknell et al., 2026). The drivers of this variability are not obvious from the present data, though foundation age and structural complexity have been suggested as contributing factors at jacket foundations in the Moray Firth (Bicknell et al., 2025).

4.2 Diel patterns in fish abundance

The Cuttlefish landers recorded pronounced diel variation in fish abundance at both distances from turbine foundations, with both haddock and flatfish showing substantially higher abundance during nocturnal and crepuscular periods than during the day. These patterns were broadly consistent across all six turbines. Haddock exhibited a sharp increase in abundance around dusk, with peak values sustained through the night and into dawn before declining after sunrise (Fig. 7). Predicted mean count at 30 m was 8.0 at night compared to 0.9 during the day; the same pattern was evident at 500 m but at lower abundances throughout (night: 3.8; day: 0.4). This nocturnal increase contrasts with diel patterns for haddock, where higher daytime counts have been reported from baited camera surveys in the North Sea (Martinez et al., 2011).

Such methods rely on active foraging responses to bait, and the contrasting pattern observed here using unbaited cameras may reflect a fundamental difference in what is being measured. A comparable nocturnal increase in water-column activity has, however, been recorded using unbaited acoustic methods at a North Sea oil and gas platform, where biological activity was higher at night (Ibanez-Erquiaga et al., 2025). Crepuscular feeding movements have also been documented for Atlantic cod at Belgian wind farm foundations, with peak activity close to sunset and sunrise (Reubens et al., 2014), though that pattern was crepuscular rather than sustained through the night as observed here for haddock.

Flatfish revealed a similar nocturnal increase but with a higher daytime baseline than haddock (Fig. 8). Predicted mean count at 30 m was 5.5 during the day and 8.5 at night. The higher daytime baseline likely reflects the benthic habit of flatfish, with individuals resting on the seabed detectable regardless of activity state. This daytime detectability is consistent with reports of higher daytime counts of common dab from both baited camera surveys (Martinez et al., 2011) and bottom trawl surveys in the North Sea (Petrakis et al., 2001). Dusk is relatively short at this latitude in July and hence results should be interpreted cautiously given limited sample sizes and durations.

The use of white light at 25% intensity is a potential confounding factor. Artificial lighting is widely recognised as a source of bias in underwater visual surveys, with behavioural responses varying between species and ranging from attraction to avoidance depending on light intensity, wavelength, and ecological context (Marchesan et al., 2005; Rooper et al., 2015; Ryer et al., 2009). At the depths sampled in the present study, ambient light levels can be reduced even during daytime, and during the nocturnal period the Cuttlefish white lights are the only light source on the seabed. The relative conspicuousness of the lights, and therefore any attraction or avoidance effect, would consequently be greater at night than during the day, which could contribute to the observed nocturnal increase in fish counts independently of any change in ambient fish abundance or behaviour. It is not possible to determine from the present data whether the nocturnal increase reflects genuine higher abundance, a behavioural response to light, or a combination of both. The Cuttlefish systems are also equipped with red light illumination, and future deployments using red light, to which many fish species are less visually sensitive, could help isolate the influence of illumination.

4.3 Comparison of baited and unbaited camera systems

BRUVs detected approximately four times more haddock and 2.6 times more flatfish than Cuttlefish landers within a 30-minute daytime window at 30 m from turbine foundations (Table 7). Higher MaxNs from baited relative to unbaited underwater video systems are well established (Harvey et al., 2007; Watson et al., 2005) and the magnitude of the difference observed here is consistent with the broader literature. Current speed was included as a covariate in the comparison models but was not significant for either species, providing confidence that the difference reflects the effect of bait rather than the environment. The two systems also differed in camera configuration, field of view, and sample size (24 BRUV deployments versus 6 Cuttlefish), and these factors may contribute to the observed differences alongside the bait effect. Both systems were artificially illuminated, so the comparison is not confounded by the presence or absence of light, although the two differed in light output.

The two systems also differed in the apparent magnitude of the distance effect. The concurrent BRUV survey estimated approximately 1.5 to 1.6 times more individuals at 30 m than at 240 m for both haddock and flatfish (Bicknell et al., 2026); whereas the daytime distance ratios from the Cuttlefish data were higher, at 2.2 for haddock and 1.9 for flatfish (Table 5). The two estimates are not directly equivalent. The far-field distances differ: Cuttlefish landers were deployed at 500 m compared to 240 m for BRUVs, so the Cuttlefish baseline encompasses a greater spatial separation from the structure and therefore a likely greater decline in its influence. The BRUV survey was also conducted during daylight, so the daytime Cuttlefish ratios provide the appropriate comparison; the full diel cycle sampled by the Cuttlefish landers, including the high-abundance nocturnal periods, would yield larger ratios still. The broadly comparable direction and magnitude of the distance effect across the two methods, despite these differences, reinforces the finding of localised aggregation near the foundations.

Both systems nevertheless detected the same spatial pattern of higher abundance near turbine foundations, indicating that the reef effect is robust to survey method. The diel patterns documented in 3.3, which would not have been captured by standard daytime BRUV deployments, illustrate the additional ecological information that extended unbaited deployments can provide.

4.4 Methodological considerations

The primary analysis used mean count derived from the automated detection model rather than MaxN from manual annotation. Mean count, calculated across all sampled frames of the full recording, makes use of the entire deployment rather than a single two-minute sample per hour, and so provides higher temporal resolution for characterising fine-scale variation in abundance through the diel cycle. The continuous values, with a high proportion of zeros, was well suited to the Tweedie distribution used in the models. As a time integrated measure, mean count reflects both the number of individuals present and the duration for which they remain in view, and where residency varies through the diel cycle this would contribute to the observed diel differences alongside any change in abundance. While automated approaches increase frequency of available for analysis, consideration should be shown to the potential for autocorrelated data series. As such, future analyses may consider the use of autocorrelation terms in their model structures. Alternatively, sub-sampling high resolution timeseries such as those created here may yield estimates with greater sample independence. The independent manual MaxN analysis, which is not influenced by residency time, recovered the same spatial and diel patterns in both direction and magnitude (3.4), providing confidence that the automated detections reflect genuine ecological signal rather than artefacts of the detection model. The distance ratios from the manual analysis were consistently lower than those from the mean count analysis, as expected given that MaxN records only the single most populated frame and therefore compresses variation relative to a measure integrated across the full deployment. The close agreement between the two approaches, despite their different metrics and sampling intensities, supports the use of automated mean count as the primary measure of abundance, with appropriate checks for autocorrelation to limit such effects.

White light at 25% intensity was selected for all deployments to provide sufficient illumination for accurate species identification while minimising battery depletion and potential behavioural disturbance. Initial quality control of the Cuttlefish footage revealed solar infrared light contamination during daylight hours on bright sunny days, with images captured between approximately 10:00 and 16:00 most affected (Fig. 10). The Cuttlefish cameras were developed without IR filters to maximise sensitivity under red light conditions. While visually distracting, the IR contamination did not prevent accurate species identification or MaxN quantification, as the outline and movement characteristics of haddock and flatfish remained sufficiently distinct for reliable counting. Automated IR filter systems coupled to external light choice have since been developed in collaboration with Inkfish to address this issue for future deployments using both white and red light configurations.

All 12 Cuttlefish landers deployments were successfully recovered, with 7 of the 12 acoustic releases activating on the first command. Deployments ranged from 14.5 to 23.2 hours, which was sufficient to capture one full diel cycle encompassing daytime, crepuscular, and nocturnal periods. The Cuttlefish systems have a battery capacity of 48 hours when recording continuously, meaning that deployments spanning multiple diel cycles are feasible and would allow assessment of day-to-day variability in fish abundance patterns at individual turbines.

4.5 Implications and conclusions

The results of this study highlight the extent to which current understanding of fish–turbine associations in the North Sea are shaped by the temporal constraints of conventional survey methods. Most published assessments of the reef effect at offshore wind farms, including the concurrent BRUV survey at Beatrice, are based on daytime deployments of relatively short duration (Bicknell et al., 2026). The diel patterns documented here suggest that such surveys capture only a portion of the fish activity occurring around turbine foundations, with nocturnal and crepuscular abundance of both haddock and flatfish substantially exceeding daytime levels. This does not invalidate daytime survey data, which remain the standard basis for spatial comparisons, but it does indicate that assessments based solely on daytime observations may underestimate the degree to which fish utilise foundation structures.

The sample size and temporal coverage of the present study, six turbines over a single week in July, limit the generality of the findings. Seasonal variation in fish abundance and diel behaviour, inter-annual variability, and the influence of foundation age and fouling community development on aggregation patterns all remain uncharacterised at this site. The confounding effect of white light on nocturnal counts, discussed in 4.2, limits the confidence with which absolute abundance comparisons between day and night can be interpreted. The patterns reported here require confirmation through repeated and expanded deployments before broader conclusions can be drawn.

References

Bates, D., Mächler, M., Bolker, B., & Walker, S. (2015). Fitting Linear Mixed-Effects Models Using-lme4. *Journal of Statistical Software*, *67*. https://doi.org/10.18637/jss.v067.i01

Bergström, L., Sundqvist, F., & Bergström, U. (2013). Effects of an offshore wind farm on temporal and spatial patterns in the demersal fish community. *Marine Ecology Progress Series*, *485*, 199-210. https://doi.org/10.3354/meps10344

Bicknell, A. W. J., Gierhart, S., Lambrette, M., & Witt, M. J. (2026). Fine-scale proximity to offshore wind turbine foundations increases biomass of demersal fish species [Original Research]. *Frontiers in Marine Science*, *Volume 13 - 2026*. https://doi.org/10.3389/fmars.2026.1765872

Bicknell, A. W. J., Gierhart, S., & Witt, M. J. (2025). Site and species dependent effects of offshore wind farms on fish populations. *Marine Environmental Research*, *205*, 106977. https://doi.org/10.1016/j.marenvres.2025.106977

Bicknell, A. W. J., Sheehan, E. V., Godley, B. J., Doherty, P. D., & Witt, M. J. (2019). Assessing the impact of introduced infrastructure at sea with cameras: A case study for spatial scale, time and statistical power. *Marine Environmental Research*, *147*, 126-137. https://doi.org/10.1016/j.marenvres.2019.04.007

Brooks, M. E., Kristensen, K., van Benthem, K. J., Magnusson, A., Berg, C. W., Nielsen, A.,…Bolker, B. M. (2017). *glmmTMB Balances Speed and Flexibility Among Packages for Zero-inflated Generalized Linear Mixed Modeling*. In CRAN. https://cran.r-project.org/web/packages/glmmTMB/index.html

Buyse, J., Hostens, K., Degraer, S., De Troch, M., & Backer, A. (2022). Increased food availability at offshore wind farms affects trophic ecology of plaice Pleuronectes platessa. *Science of The Total Environment*, *862*, 160730. https://doi.org/10.1016/j.scitotenv.2022.160730

Cappo, M., Harvey, E., Malcolm, H., & Speare, P. (2003). Potential of video techniques to monitor diversity, abundance and size of fish in studies of Marine Protected Areas. *Aquatic Protected Areas-what works best and how do we know*, 455-464.

Degraer, S., Carey, D., Coolen, J., Hutchison, Z., Kerckhof, F., Rumes, B., & Vanaverbeke, J. (2020). Offshore Wind Farm Artificial Reefs Affect Ecosystem Structure and Functioning: A Synthesis. *Oceanography*, *33*, 48-57. https://doi.org/10.5670/oceanog.2020.405

Dunkley, F., & Solandt, J.-L. (2022). Windfarms, fishing and benthic recovery: Overlaps, risks and opportunities. *Marine Policy*, *145*, 105262. https://doi.org/10.1016/j.marpol.2022.105262

Engås, A., & Soldal, A. V. (1992). Diurnal variations in bottom trawl catch rates of cod and haddock and their influence on abundance indices. *ICES Journal of Marine Science*, *49*(1), 89-95. https://doi.org/10.1093/icesjms/49.1.89

Foster, S. D., & Bravington, M. V. (2013). A Poisson–Gamma model for analysis of ecological non-negative continuous data. *Environmental and Ecological Statistics*, *20*(4), 533-552. https://doi.org/10.1007/s10651-012-0233-0

Harvey, E., Cappo, M., Butler, J., Hall, N., & Kendrick, G. (2007). Bait attraction affects the performance of remote underwater video stations in assessment of demersal fish community structure. *Marine Ecology Progress Series*, *350*, 245-254. https://doi.org/10.3354/meps07192

Ibanez-Erquiaga, B., Baktoft, H., Mildenberger, T. K., Teilmann, J., Kleivane, L., Kornau, L. M.,…Svendsen, J. C. (2025). Increased fish abundance, biodiversity, and body size near a North Sea oil and gas platform. *Mar Environ Res*, *204*, 106959. https://doi.org/10.1016/j.marenvres.2025.106959

Lambrette, M., Bicknell, A. W. J., Gierhart, S., & Witt, M. J. (2026). *YOLO object detection for rapid assessment of the abundance of commercially important fish species*. University of Exeter.

Lenth, R. V., & Piaskowski, J. (2025). *emmeans: Estimated Marginal Means, aka Least-Squares Means*. In (Version 2.0.0) CRAN. https://CRAN.R-project.org/package=emmeans

Løkkeborg, S., Bjordal, Å., & Fernö, A. (1989). Responses of Cod (Gadus morhua) and Haddock (Melanogrammus aeglefinus) to Baited Hooks in the Natural Environment. *Canadian Journal of Fisheries and Aquatic Sciences*, *46*(9), 1478-1483. https://doi.org/10.1139/f89-189

Marchesan, M., Spoto, M., Verginella, L., & Ferrero, E. A. (2005). Behavioural effects of artificial light on fish species of commercial interest. *Fisheries Research*, *73*(1), 171-185. https://doi.org/10.1016/j.fishres.2004.12.009

Martinez, I., Jones, E. G., Davie, S. L., Neat, F. C., Wigham, B. D., & Priede, I. G. (2011). Variability in behaviour of four fish species attracted to baited underwater cameras in the North Sea. *Hydrobiologia*, *670*(1), 23-34. https://doi.org/10.1007/s10750-011-0672-x

Petrakis, G., MacLennan, D. N., & Newton, A. W. (2001). Day–night and depth effects on catch rates during trawl surveys in the North Sea. *ICES Journal of Marine Science*, *58*(1), 50-60. https://doi.org/10.1006/jmsc.2000.0989

Reubens, J. T., De Rijcke, M., Degraer, S., & Vincx, M. (2014). Diel variation in feeding and movement patterns of juvenile Atlantic cod at offshore wind farms. *Journal of Sea Research*, *85*, 214-221. https://doi.org/10.1016/j.seares.2013.05.005

Reubens, J. T., Pasotti, F., Degraer, S., & Vincx, M. (2013). Residency, site fidelity and habitat use of Atlantic cod (Gadus morhua) at an offshore wind farm using acoustic telemetry. *Marine Environmental Research*, *90*, 128-135. https://doi.org/10.1016/j.marenvres.2013.07.001

Reubens, J. T., Vandendriessche, S., Zenner, A. N., Degraer, S., & Vincx, M. (2013). Offshore wind farms as productive sites or ecological traps for gadoid fishes?--impact on growth, condition index and diet composition. *Mar Environ Res*, *90*, 66-74. https://doi.org/10.1016/j.marenvres.2013.05.013

Rooper, C. N., Williams, K., De Robertis, A., & Tuttle, V. (2015). Effect of underwater lighting on observations of density and behavior of rockfish during camera surveys. *Fisheries Research*, *172*, 157-167. https://doi.org/10.1016/j.fishres.2015.07.012

Ryer, C., Stoner, A., Iseri, P., & Spencer, M. (2009). Effects of simulated underwater vehicle lighting on fish behavior. *Marine Ecology Progress Series*, *391*, 97-106. https://doi.org/10.3354/meps08168

Team, R. C. (2022). *R: A Language and Environment for Statistical Computing*. In R Foundation for Statistical Computing. https://www.R-project.org/

ter Hofstede, R., Driessen, F., Elzinga, P. J., van Koningsveld, M., & Schutter, M. (2022). Offshore wind farms contribute to epibenthic biodiversity in the North Sea. *Journal of Sea Research*, *185*, 102229. https://doi.org/10.1016/j.seares.2022.102229

Thieurmel, B., & Elmarhraoui, A. (2022). *suncalc: Compute Sun Position, Sunlight Phases, Moon Position and Lunar Phase*. In (Version 0.5.1) CRAN. https://CRAN.R-project.org/package=suncalc

Watson, D. L., Harvey, E. S., Anderson, M. J., & Kendrick, G. A. (2005). A comparison of temperate reef fish assemblages recorded by three underwater stereo-video techniques. *Marine Biology*, *148*(2), 415-425. https://doi.org/10.1007/s00227-005-0090-6

Wilhelmsson, D., Malm, T., & Öhman, M. C. (2006). The influence of offshore windpower on demersal fish. *ICES Journal of Marine Science*, *63*(5), 775-784. https://doi.org/10.1016/j.icesjms.2006.02.001

Willis, T., & Babcock, R. (2000). A baited underwater video system for the determination of relative density of carnivorous reef fish. *Marine and Freshwater Research*, *51*, 755-763.

Supplementary Material

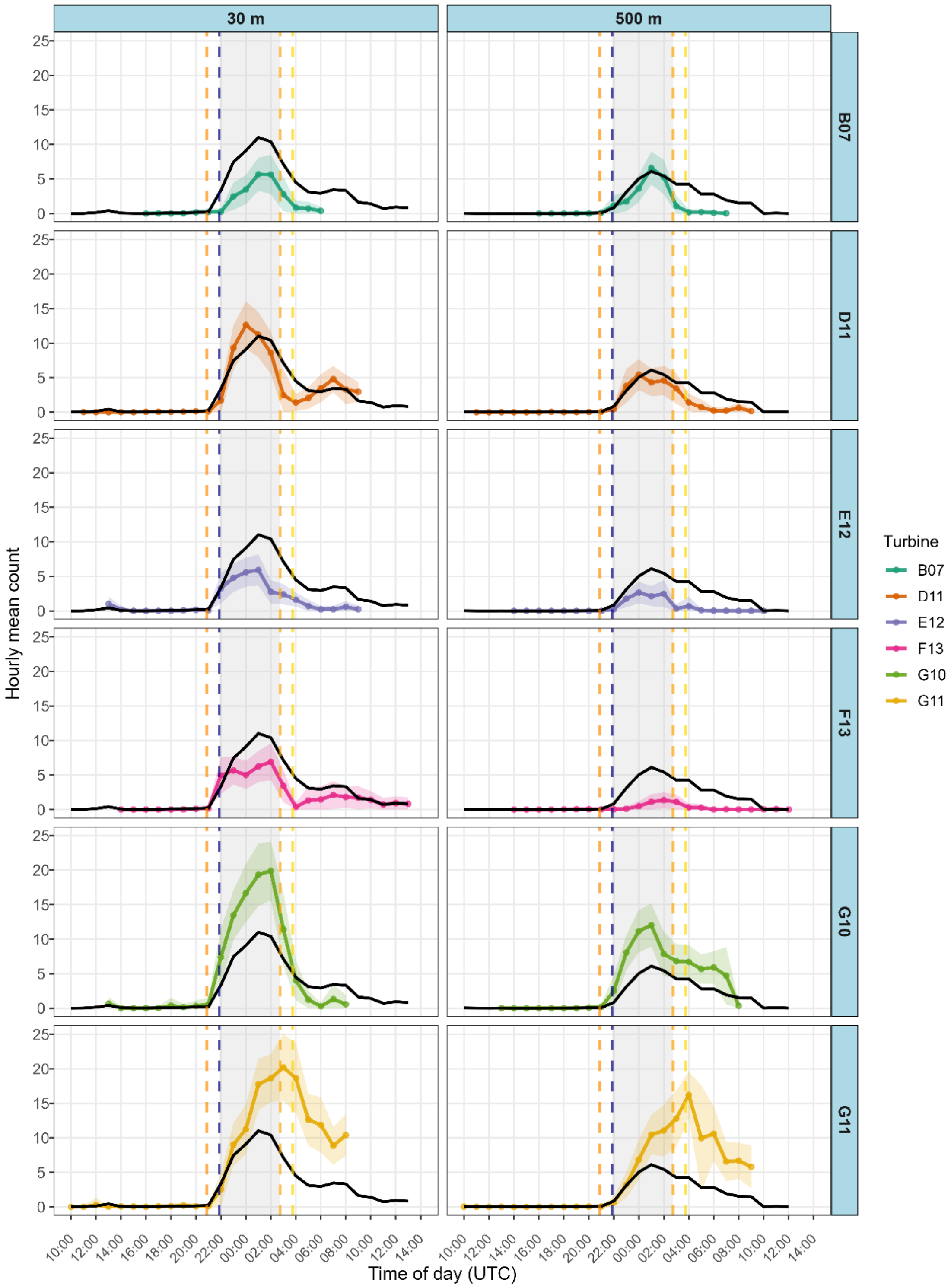

Figure S1. Hourly mean count of Gadidae through the diel cycle at each of the six turbine foundations (rows), at 30 m and 500 m from the foundation (columns). Coloured lines show the mean count for the individual turbine and the shaded band shows ±1 standard deviation across the per-frame detections within each hour. The black line shows the grand mean across all turbines for reference. Vertical dashed lines mark the dawn and dusk transitions, and the grey shaded area indicates the hours of darkness.

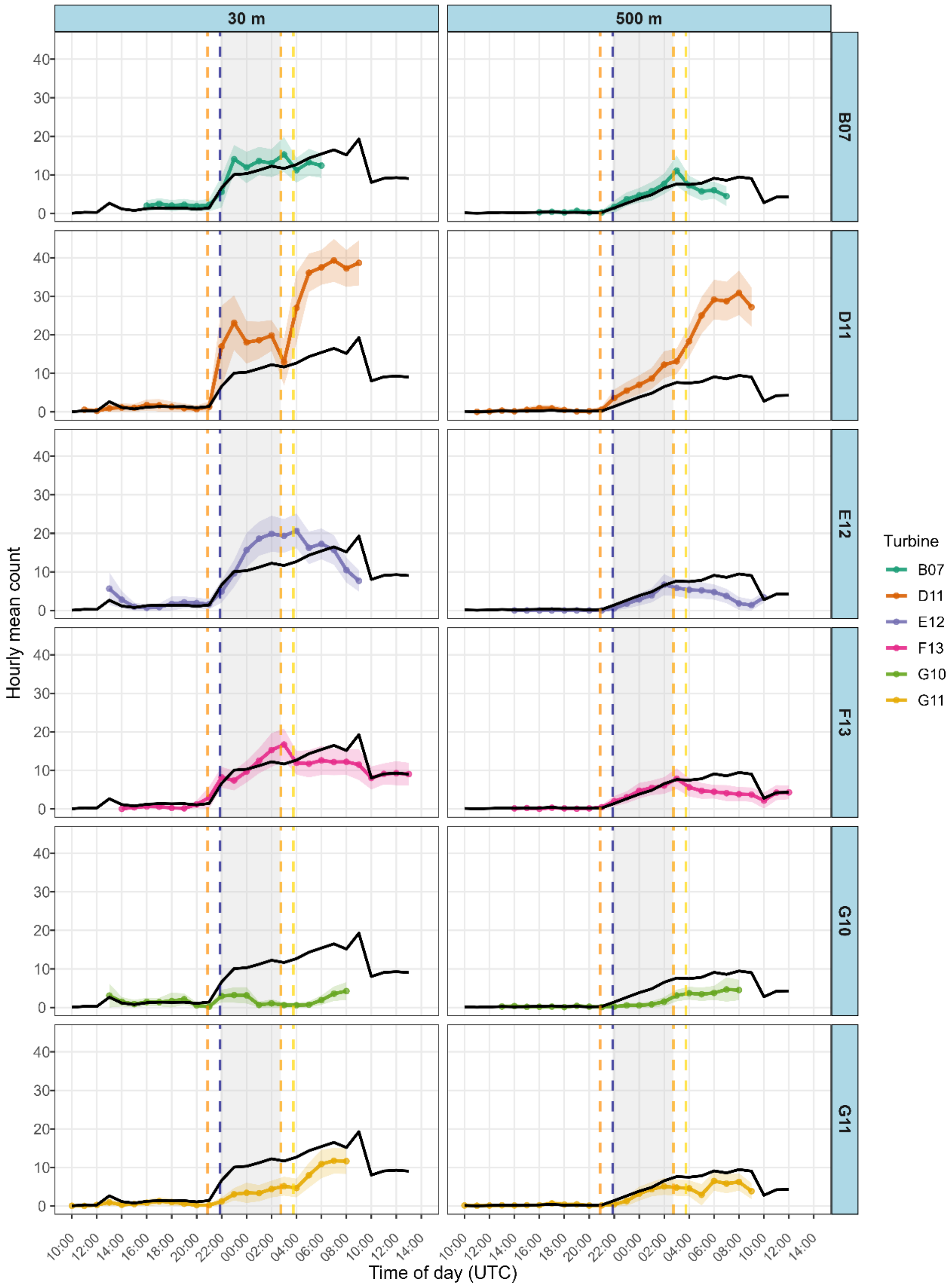

Figure S2. Hourly mean count of Pleuronectiformes through the diel cycle at each of the six turbine foundations (rows), at 30 m and 500 m from the foundation (columns). Coloured lines show the mean count for the individual turbine and the shaded band shows ±1 standard deviation across the per-frame detections within each hour. The black line shows the grand mean across all turbines for reference. Vertical dashed lines mark the dawn and dusk transitions, and the grey shaded area indicates the hours of darkness.